Inorg. Chem. **2007**, *46*, 9884–9894

Novel Manganese(II) Sulfonate–Phosphonates with Dinuclear, Tetranuclear, and Hexanuclear Clusters

Zi-Yi Du,[†] Andrey V. Prosvirin,[‡] and Jiang-Gao Mao*,[†]

State Key Laboratory of Structural Chemistry, Fujian Institute of Research on the Structure of Matter, Chinese Academy of Sciences, Fuzhou 350002, P. R., China, and Department of Chemistry, Texas A&M University, P.O. Box 30012, College Station, Texas 77843-3012

Received June 21, 2007

Hydrothermal reactions of manganese(II) salts with *m*-sulfophenylphosphonic acid (*m*-HO_3S–Ph–PO_3H_2, H_3L) and 1,10-phenanthroline (phen) led to six novel manganese(II) sulfonate–phosphonates, namely, $[Mn_2(HL)_2(phen)_4]$-$[Mn_2(HL)_2(phen)_4(H_2O)]_2 \cdot 6H_2O$ (**1**), $[Mn_4(L)_2(phen)_8(H_2O)_2][ClO_4]_2 \cdot 3H_2O$ (**2**), $[Mn(phen)(H_2O)_4]_2[Mn_4(L)_4(phen)_4] \cdot 10H_2O$ (**3**), $[Mn_6(L)_4(phen)_8(H_2O)_2] \cdot 4H_2O$ (**4**), $[Mn_6(L)_4(phen)_8(H_2O)_2] \cdot 24H_2O$ (**5**), and $[Mn_6(L)_4(phen)_6(H_2O)_4] \cdot 5H_2O$ (**6**). The structure of **1** contains two types of dinuclear manganese(II) clusters, and **2**–**3** exhibit two types of tetranuclear manganese(II) cluster units. **4**–**5** feature two different types of isolated hexanuclear manganese(II) clusters, whereas the hexanuclear manganese(II) clusters in **6** are bridged by sulfonate–phosphonate ligands into a 1D chain. Magnetic property measurements indicate that there exist weak antiferromagnetic interactions between magnetic centers in all six compounds.

Introduction

The chemistry of metal phosphonates has been a research field of rapid expansion in recent years, mainly due to their potential application in the area of catalysis, ion exchange, proton conductivity, intercalation chemistry, photochemistry, and materials chemistry.[1] Most of the metal phosphonates have a layered structure in which the metal centers are bridged by the phosphonate groups, although a variety of 1D chains and porous 3D networks have also been reported.[1] Metal phosphonates containing a molecular cluster unit are still relatively rare.[2−7] A lanthanide phosphonate cage compound with a $\{Na_6Eu_9L_{16}\}$ (H_2L = 5′-methyl-2,2′-bipy-6-phosphonic acid) core and several tetranuclear lanthanide(III)-sulfonate−phosphonates has been prepared.[2] Several cage complexes involving vanadium and aluminum have been reported.[3] Two mixed-valence polyoxomolybdenum diphosphonate anions were reported by the Sevov group.[4] Several tetranuclear, hexanuclear, heptanuclear, and nonanuclear iron(III) phosphonate cages have been isolated.[5] A few cobalt phosohonate cages were also synthesized.[6] A variety of zinc(II) clusters ranging from trinuclear, tetra-

* To whom correspondence should be addressed. mjg@fjirsm.ac.cn.
[†] Fujian Institute of Research on the Structure of Matter.
[‡] Texas A&M University.

(1) (a) Clearfield, A. Metal Phosphonate Chemistry In *Progress in Inorganic Chemistry*; Karlin, K. D., Ed.; John Wiley & Sons: New York, 1998, *47*, pp 371−510 (and references therein). (b) Maeda, K. *Microporous Mesoporous Mater.* **2004**, *73*, 47 (and references therein). (c) Mao, J.-G. *Coord. Chem. Rev.* **2007**, *251*, 1493 (and references therein).
(2) (a) Comby, S.; Scopelliti, R.; Imbert, D.; Charbonniere, L.; Ziessel, R.; Bunzli, J.-C. G. *Inorg. Chem.* **2006**, *45*, 3158. (b) Du, Z.-Y.; Xu, H.-B.; Mao, J.-G. *Inorg. Chem.* **2006**, *45*, 9780.
(3) (a) Khan, M. I.; Zubieta, J. *Prog. Inorg. Chem.* **1995**, *43*, 1 (and references therein). (b) Walawalker, M. G.; Roesky, H. W.; Murugavel, R. *Acc. Chem. Res.* **1999**, *32*, 117 (and references therein).
(4) Dumas, E.; Sassoye, C.; Smith, K. D.; Sevov, S. C. *Inorg. Chem.* **2002**, *41*, 4029.
(5) (a) Konar, S.; Bhuvanesh, N.; Clearfield, A. *J. Am. Chem. Soc.* **2006**, *128*, 9604. (b) Tolis, E. I.; Engelhardt, L. P.; Mason, P. V.; Rajaraman, G.; Kindo, K.; Luban, M.; Matsuo, A.; Nojiril, H.; Raftery, J.; Schroder, C.; Timco, G. A.; Tuna, F.; Wernsdorfer, W.; Winpenny, R. E. P. *Chem.—Eur. J.* **2006**, *12*, 8961. (c) Yao, H. C.; Wang, J.-J.; Ma, Y.-S.; Waldmann, O.; Du, W. X.; Song, Y.; Li, Y.-Z.; Zheng, L.-M.; Decurtins, S.; Xin, X.-Q. *Chem. Commun.* **2006**, 1745. (d) Tolis, E. I.; Helliwell, M.; Langley, S.; Raftery, J.; Winpenny, R. E. P. *Angew. Chem., Int. Ed.* **2003**, *42*, 3804. (e) Yao, H. C.; Li, Y.-Z.; Zheng, L.-M.; Xin, X.-Q. *Inorg. Chim. Acta* **2005**, *358*, 2523.
(6) (a) Langley, S. J.; Helliwell, M.; Sessoli, R.; Rosa, P.; Wernsdorfer, W.; Winpenny, R. E. P. *Chem. Commun.* **2005**, 5029. (b) Brechin, E. K.; Coxall, R. A.; Parkin, A.; Parsons, S.; Tasker, P. A.; Winpenny, R. E. P. *Angew. Chem., Int. Ed.* **2001**, *40*, 2700.
(7) (a) Chandrasekhar, V.; Kingsley, S. *Angew. Chem., Int. Ed.* **2000**, *39*, 2320. (b)Yang, Y.; Pinkas, J.; Noltemeyer, M.; Schmidt, H.-G.; Roesky, H. W. *Angew. Chem., Int. Ed.* **1999**, *38*, 664. (c) Chandrasekhar, V.; Kingsley, S.; Rhatigan, B.; Lam, M. K.; Rheingold, A. L. *Inorg. Chem.* **2002**, *41*, 1030. (d) Chandrasekhar, V.; Sasikumar, P.; Boomishankar, R.; Anantharaman, G. *Inorg. Chem.* **2006**, *45*, 3344. (e) Lei, C.; Mao, J.-G.; Sun, Y.-Q.; Zeng, H.-Y.; Clearfield, A. *Inorg. Chem.* **2003**, *42*, 6157. (f) Yang, B.-P.; Mao, J.-G.; Sun, Y.-Q.; Zhao, H.-H.; Clearfield, A. *Eur. J. Inorg. Chem.* **2003**, 4211. (g) Cao, D.-K.; Li, Y.-Z.; Zheng, L.-M. *Inorg. Chem.* **2005**, *44*, 2984. (h) Du, Z.-Y.; Xu, H.-B.; Mao, J.-G. *Inorg. Chem.* **2006**, *45*, 6424.

10.1021/ic701213g CCC: $37.00
Published on Web 10/06/2007

nuclear, hexanuclear, heptanuclear to dodecanuclear have been structurally characterized.[7]

Manganese cluster compounds are of great research interest because of their biological relevance as models of active sites in metal enzymes and their unusual magnetic behavior such as their ability to function as single molecule magnets.[8,9] Although a large number of manganese phosphonates have been reported,[10−12] only a few of them contain isolated cluster units.[12] Several manganese(III) or mixed-valent manganese cage compounds ranging from Mn_6 to Mn_{20} were obtained by Winpenny et al. by the reaction of a phosphonic acid with a mixed-valent trinuclear cluster such as $[Mn_3O(L)_6(py)_{3-x}(H_2O)_x]$ (L = $PhCO_2$ or Me_3CCO_2; $x = 0$ or 1).[12a−c] It is found that minor changes in phosphonate ligands or solvents can lead to completely different cluster cores. Tetranuclear mixed-valent (manganese(II)/manganese(III)) cage compounds have been obtained by the direct reaction of manganese(II) salt with phosphonic acid in the presence of small amount of pyridine as a base.[12d] The four manganese centers form a tetrahedron. By using manganese(II) and manganese(VII) as the manganese sources, carboxylate and phosphonate as metal linkers and bidentate chelating phen or bipy as the auxiliary ligand, tetranuclear and dodecanuclear manganese(III) phosphonate cage compounds were prepared by Zheng, et al.[12e,12f] So far, no metal phosphonate cage compounds based purely on manganese(II) centers have been reported.

We have successfully developed a new route for the preparations of transition-metal or lanthanide phosphonate cluster compounds.[2b,7h] Our strategy is attaching a weak-coordination sulfonate group to the phosphonic acid and selecting a suitable second metal linker. A weak-coordination sulfonate group attached on a phosphonic acid can not only increase the solubility of the metal phosphonates formed but also provide a hindrance for the formation of the extended structures. Furthermore, the introduction of an auxiliary ligand such as 1,10-phenanthroline could reduce the coordination sites available for the phosphonate ligand and thereby facilitates the formation of cluster compounds. Extending such a synthetic technique to the manganese(II) system afforded six novel manganese(II) sulfonate−phosphonate clusters, namely, $[Mn_2(HL)_2(phen)_4][Mn_2(HL)_2(phen)_4(H_2O)]_2\cdot 6H_2O$ (**1**), $[Mn_4(L)_2(phen)_8(H_2O)_2][ClO_4]_2\cdot 3H_2O$ (**2**), $[Mn(phen)(H_2O)_4]_2[Mn_4(L)_4(phen)_4]\cdot 10H_2O$ (**3**), $[Mn_6(L)_4(phen)_8(H_2O)_2]\cdot 4H_2O$ (**4**), $[Mn_6(L)_4(phen)_8(H_2O)_2]\cdot 24H_2O$ (**5**), and $[Mn_6(L)_4(phen)_6(H_2O)_4]\cdot 5H_2O$ (**6**). Herein, we report their syntheses, crystal structures, and magnetic properties.

Experimental Section

Materials and Instrumentations. *m*-Sulfophenylphosphonic acid (m-$HO_3S-C_6H_4-PO_3H_2$, H_3L) was synthesized according to the procedures previously described by Montoneri.[7h,13] All of the other chemicals were obtained from commercial sources and used without further purification. Elemental analyses were performed on a German Elementary Vario EL III instrument. The FTIR spectra were recorded on a Nicolet Magna 750 FTIR spectrometer using KBr pellets in the range of 4000−400 cm^{-1}. Thermogravimetric analyses were carried out on a NETZSCH STA 449C unit at a heating rate of 10 °C/min under an oxygen atmosphere. X-ray powder diffraction (XRD) patterns (Cu Kα) were collected on a PANalytical X'Pert Pro $\theta-2\theta$ diffractometer. Magnetic susceptibility measurements were carried out on a Quantum Design MPMS-XL SQUID magnetometer. The raw data were corrected for the susceptibility of the container and the diamagnetic contributions of the sample using Pascal constants.

Syntheses of $[Mn_2(HL)_2(phen)_4][Mn_2(HL)_2(phen)_4(H_2O)]_2\cdot 6H_2O$ (1) and $[Mn(phen)(H_2O)_4]_2[Mn_4(L)_4(phen)_4]\cdot 10H_2O$ (3). The two compounds were synthesized in a similar method. For the preparation of **1**, a mixture of $Mn(ac)_2$ (0.3 mmol), H_3L (0.3 mmol), and phen (0.45 mmol) in 10 mL distilled water with its pH value adjusted to 3.2 by the addition of 1M NaOH solution and was put into a Parr Teflon-lined autoclave (23 mL) and heated at 150 °C for 4 days. Brick-shaped yellow crystals of **1** were collected in a ca. 52% yield based on manganese. Applying a $Mn(ac)_2/H_3L$/phen molar ratio of 0.3:0.24:0.3, and the initial pH value of 5.4 afforded plate-shaped yellow crystals of **3** in a ca. 56% yield (based on manganese). Their purities have also been confirmed by XRD powder diffraction studies (Figure S1 in the Supporting Information). Anal. Calcd for **1** ($C_{180}H_{142}N_{24}O_{44}P_6S_6Mn_6$, Mr = 4053.00): C, 53.34; H, 3.53; N, 8.29; Found: C, 53.08; H, 3.59; N, 8.14; for **3** ($C_{96}H_{100}N_{12}O_{42}P_4S_4Mn_6$, Mr = 2675.64): C, 43.09; H, 3.77; N, 6.28. Found: C, 43.20; H, 3.83; N, 6.39. IR data (KBr, cm^{-1}) for **1**: 3445(s), 3064(m), 2913(m), 1625(m), 1517(m), 1425(s), 1219(s), 1187(vs), 1101(vs), 1064(s), 1031(vs), 906(m), 849(m), 796(m), 730(s), 688(m), 618(m), 561(m); for **3**: 3434(s), 3059(m), 2918(m), 1625(m), 1518(m), 1426(s), 1161(s), 1102(vs), 1033(vs), 999(m), 848(m), 792(m), 729(s), 619(m), 553(m).

(8) (a) Weinheim, V. C. H. *Manganese Redox Enzymes*; Pecoraro, V. L., Ed., 1992. (b) Ferreira, K. N.; Iverson, T. M.; Maghlaoui, K.; Barber, J.; Iwata, S. *Science* **2004**, *303*, 1831. (c) Mishra, A.; Wernsdorfer, W.; Abboud, K. A.; Christou, G. *Chem. Commun.* **2005**, 54.

(9) (a) Sessoli, R.; Gatteschi, D.; Caneschi, A.; Novak, M. A. *Nature* **1993**, *365*, 141. (b) Aubin, S. M. J.; Dilley, N. R.; Wemple, M. W.; Maple, M. B.; Christou, G.; Hendrickson, D. N. *J. Am. Chem. Soc.* **1998**, *120*, 839. (c) Gatteschi, D.; Sessoli, R. *Angew. Chem., Int. Ed.* **2003**, *42*, 268.

(10) (a) Mao, J.-G.; Wang, Z.-K.; Clearfield, A. *Inorg. Chem.* **2002**, *41*, 2334. (b) Yang, B.-P.; Mao, J.-G. *Inorg. Chem.* **2005**, *44*, 5661. (c) Sun, Z.-M.; Mao, J.-G.; Dong, Z.-C. *Polyhedron* **2005**, *24*, 571. (d) Bao, S. S.; Chen, G.-S.; Wang, Y.; Li, Y.-Z.; Zheng, L.-M.; Luo, Q.-H. *Inorg. Chem.* **2006**, *45*, 1124. (e) Yin, P.; Gao, S.; Wang, Z.-M.; Yan, C.-H.; Zheng, L.-M.; Xin, X.-Q. *Inorg. Chem.* **2005**, *44*, 2761. (f) Song, H.-H.; Yin, P.; Zheng, L.-M.; Korp, J. D.; Jacobson, A.-J.; Gao, S.; Xin, X.-Q. *J. Chem. Soc., Dalton Trans.* **2002**, 2752.

(11) (a) Stock, N.; Frey, S. A.; Stucky, G.-D.; Cheetham, A. K. *J. Chem. Soc., Dalton Trans.* **2000**, 4292. (b) Cabeza, A.; Aranda, M. A. G.; Bruque, S.; Poojary, D. M.; Clearfield, A. *Mater. Res. Bull.* **1998**, *33*, 1265. (c) Cabeza, A.; Ouyang, X.; Sharma, C. V. K.; Aranda, M. A. G.; Bruque, S.; Clearfield, A. *Inorg. Chem.* **2002**, *41*, 2325. (d) Stock, N.; Bein, T. *J. Solid State Chem.* **2002**, *167*, 330. (e) Ayyappan, P.; Evans, O. R.; Cui, Y.; Wheeler, K. A.; Lin, W. B. *Inorg. Chem.* **2002**, *41*, 4978. (f) Stock, N.; Karaghiosoff, K.; Bein, T. *Z. Anorg. Allg. Chem.* **2004**, *630*, 2535. (g) Stock, N.; Bein, T. *J. Mater. Chem.* **2005**, *15*, 1384. (h) Tsao, C.-P.; Sheu, C.-Y.; Nguyen, N.; Lii, K.-H. *Inorg. Chem.* **2006**, *45*, 6361.

(12) (a) Maheswaran, S.; Chastanet, G.; Teat, S. J.; Mallah, T.; Sessoli, R.; Wernsdorfer, W.; Winpenny, R. E. P. *Angew. Chem., Int. Ed.* **2005**, *44*, 5044. (b) Shanmugam, M.; Chastanet, G.; Mallah, T.; Sessoli, R.; Teat, S. J.; Timco, G. A.; Winpenny, R. E. P. *Chem.—Eur. J.* **2006**, *12*, 8777. (c) Shanmugam, M.; Shanmugam, M.; Chastanet, G.; Sessoli, R.; Mallah, T.; Wernsdorfe, W.; Winpenny, R. E. P. *J. Mater. Chem.* **2006**, *16*, 2576. (d) Baskar, V.; Shanmugam, M.; Sañudo, E. C.; Shanmugam, M.; Collison, D.; McInnes, E. J. L.; Wei, Q.; Winpenny, R. E. P. *Chem. Commun.* **2007**, 37. (e) Yao, H.-C.; Li, Y.-Z.; Song, Y.; Ma, Y.-S.; Zheng, L.-M.; Xin, X.-Q. *Inorg. Chem.* **2006**, *45*, 59. (f) Ma, Y.-S.; Yao, H.-C.; Hua, W.-J.; Li, S.-H.; Li, Y.-Z.; Zheng, L.-M. *Inorg. Chim. Acta* **2007**, *360*, 1645.

(13) (a) Montoneri, E. *Phosphorus, Sulfur Silicon, Relat. Elem.* **1991**, *55*, 201. (b) Montoneri, E.; Gallazzi, M. C. *Dalton Trans.* **1989**, 1819.

Table 1. Summary of Crystal Data and Structural Refinements for **1**–**6**

compound	**1**	**2**	**3**	**4**	**5**	**6**
formula	$C_{180}H_{142}N_{24}O_{44}P_6S_6Mn_6$	$C_{108}H_{82}Cl_2N_{16}O_{25}P_2S_2Mn_4$	$C_{96}H_{100}N_{12}O_{42}P_4S_4Mn_6$	$C_{120}H_{92}N_{16}O_{30}P_4S_4Mn_6$	$C_{120}H_{132}N_{16}O_{50}P_4S_4Mn_6$	$C_{96}H_8N_{12}O_{33}P_4S_4Mn_6$
fw	4053.00	2420.62	2675.64	2819.86	3180.18	2513.50
space group	$P\bar{1}$	$P2_1/c$	$P\bar{1}$	$P\bar{1}$	$P\bar{1}$	$P\bar{1}$
a (Å)	14.533(2)	15.352(3)	13.232(2)	14.6347(1)	14.092(3)	15.987(3)
b (Å)	15.438(2)	13.628(3)	13.868(2)	15.1733(3)	16.076(3)	16.587(3)
c (Å)	22.174(3)	26.195(6)	17.727(3)	16.2370(3)	16.124(3)	19.414(3)
α (deg)	83.964(5)	90	84.144(7)	112.272(1)	73.799(5)	82.378(4)
β (deg)	79.984(5)	102.030(3)	69.201(5)	93.13	87.716(7)	80.176(3)
γ (deg)	64.913(4)	90	67.703(6)	114.910(1)	73.791(6)	85.986(4)
V (Å^3)	4434(1)	5360(2)	2811.4(8)	2925.92(8)	3365(1)	5022(1)
Z	1	2	1	1	1	2
D_{calcd} (g cm^{-3})	1.518	1.500	1.580	1.600	1.569	1.662
μ (mm^{-1})	0.628	0.662	0.877	0.841	0.751	0.970
GOF on F^2	1.036	1.068	1.040	1.099	1.061	1.075
R1, wR2 [$I > 2\sigma(I)$]^a	0.0612, 0.1684	0.0758, 0.2296	0.0459, 0.1193	0.0321, 0.0793	0.0609, 0.1454	0.0557, 0.1363
R1, wR2 (all data)^a	0.0707, 0.1783	0.0935, 0.2507	0.0591, 0.1299	0.0392, 0.0869	0.0763, 0.1594	0.0846, 0.1567

^{a} $R1 = \sum||F_o| - |F_c||/\sum|F_o|$, $wR2 = \{\sum w[(F_o)^2 - (F_c)^2]^2/\sum w[(F_o)^2]^2\}^{1/2}$.

Syntheses of $[Mn_4(L)_2(phen)_8(H_2O)_2][ClO_4]_2\cdot 3H_2O$ (2) and $[Mn_6(L)_4(phen)_6(H_2O)_4]\cdot 5H_2O$ (6). These two compounds were synthesized by a similar procedure. A mixture of $Mn(ClO_4)_2$ (0.3 mmol), H_3L (0.3 mmol), and phen (0.5 mmol) in 10 mL distilled water with its pH value adjusted to 2.9 by the addition of 1M NaOH solution was put into a Parr Teflon-lined autoclave (23 mL) and heated at 150 °C for 3 days. Plate-shaped yellow crystals of **2** were collected in a ca. 68% yield based on manganese. Using a $Mn(ClO_4)_2/H_3L$/phen molar ratio of 0.3:0.3:0.3 and the initial pH value of 3.7, brick-shaped yellow crystals of **6** were collected in a ca. 60% yield (based on manganese). Their purities have also been confirmed by XRD powder diffraction studies (Figure S1 in the Supporting Information). Anal. Calcd for **2** ($C_{108}H_{82}Cl_2N_{16}O_{25}P_2S_2Mn_4$, $Mr = 2420.62$): C, 53.59; H, 3.41; N, 9.26. Found: C, 53.41; H, 3.63; N, 9.12; for **6** ($C_{96}H_8N_{12}O_{33}P_4S_4Mn_6$, $Mr = 2513.50$): C, 45.86; H, 3.29; N, 6.69. Found: C, 45.92; H, 3.17; N, 6.62. IR data (KBr, cm^{-1}) for **2**: 3430(s), 3061(m), 2913(m), 1624(m), 1517(m), 1425(s), 1195(s), 1101(vs), 1032(vs), 1001(m), 844(m), 797(m), 729(s), 698(m), 623(m), 573(m); for **6**: 3435(s), 3069(m), 2924(m), 1624(m), 1518(m), 1425(s), 1217(s), 1178(vs), 1149(vs), 1123(vs), 1101(vs), 1032(vs), 999(s), 851(m), 795(s), 730(m), 692(m), 621(m), 554(m).

Syntheses of $[Mn_6(L)_4(phen)_8(H_2O)_2]\cdot 4H_2O$ (4) and $[Mn_6(L)_4(phen)_8(H_2O)_2]\cdot 24H_2O$ (5). Both compounds were synthesized using $MnSO_4$ as the manganese source. A mixture of $MnSO_4$ (0.36 mmol), H_3L (0.36 mmol), and phen (0.45 mmol) in 10 mL distilled water with its pH value adjusted to 5.1 by the addition of a 1M NaOH solution, was put into a Parr Teflon-lined autoclave (23 mL) and heated at 140 °C for 3 days. Brick-shaped yellow crystals of **4** were collected in a ca. 63% yield based on manganese. With a same M/L/phen molar ratio at a slightly lower pH value of 4.2, brick-shaped yellow crystals of **5** were collected in a ca. 66% yield based on manganese. Their purities have also been confirmed by XRD powder diffraction studies (Figure S1 in the Supporting Information). Anal. Calcd for **4** ($C_{120}H_{92}N_{16}O_{30}P_4S_4Mn_6$, $Mr = 2819.86$): C, 51.11; H, 3.29; N, 7.95. Found: C, 50.91; H, 3.56; N, 7.91; for **5** ($C_{120}H_{132}N_{16}O_{50}P_4S_4Mn_6$, $Mr = 3180.18$): C, 45.31; H, 4.19; N, 7.05. Found: C, 45.33; H, 4.66; N, 7.07. IR data (KBr, cm^{-1}) for **4**: 3434(s), 3059(m), 2921(m), 1624(m), 1518(m), 1426(s), 1223(s), 1186(vs), 1150(vs), 1133(vs), 1101(vs), 1064(s), 1032(vs), 1012(s), 956(s), 848(m), 798(m), 730(s), 699(m), 619(m), 522(m); for **5**: 3433(s), 3064(m), 2924(m), 1625(m), 1517(m), 1425(s), 1220(s), 1186(vs), 1142(vs), 1100(vs), 1032(vs), 1000(s), 847(m), 729(s), 700(m), 620(m), 555(m).

Single-Crystal Structure Determination. Data collections were performed on a Mercury CCD diffractometer (for **1** and **3**) or a Saturn 70 CCD diffractometer (for **2**, **5**, and **6**) or a Siemens Smart CCD diffractometer (for **4**). All of the diffractometers were equipped with a graphite monochromated Mo Kα radiation ($\lambda = 0.71073$ Å). Data collection for **5** was performed at 123 K, whereas those for the remaining five were performed under room temperature. These data sets were corrected for Lorentz and polarization factors as well as for absorption by the *SADABS* program or Multiscan Method.[14a,14b] All of the structures were solved by the direct method and refined by full-matrix least-squares fitting on F^2 by *SHELX-97*.[14c] All of the non-hydrogen atoms except oxygen atoms of the ClO_4^- group in **2** were refined with anisotropic thermal parameters. All of the hydrogen atoms were generated geometrically and refined isotropically.

(14) (a) Sheldrick, G. M. *Program SADABS*; Universität Göttingen: Göttingen, Germany, 1995. (b) *CrystalClear*, version 1.3.5; Rigaku Corp.: Woodlands, TX, 1999. (c) Sheldrick, G. M. *SHELX-96, Program for Crystal Structure Determination*; 1996.

Table 2. Selected Bond Lengths (Å) for **1**−**6**[a]

1			
Mn(1)−O(2)#1	2.066(2)	Mn(1)−O(1)	2.097(2)
Mn(1)−N(4)	2.253(2)	Mn(1)−N(1)	2.262(3)
Mn(1)−N(2)	2.316(3)	Mn(1)−N(3)	2.341(3)
Mn(2)−O(9)	2.083(2)	Mn(2)−O(14)	2.111(2)
Mn(2)−N(5)	2.277(2)	Mn(2)−N(8)	2.281(2)
Mn(2)−N(7)	2.286(2)	Mn(2)−N(6)	2.345(3)
Mn(3)−O(8)	2.066(2)	Mn(3)−O(1W)	2.182(3)
Mn(3)−N(12)	2.266(3)	Mn(3)−N(10)	2.267(3)
Mn(3)−N(9)	2.310(3)	Mn(3)−N(11)	2.318(3)
P(1)−O(2)	1.495(2)	P(1)−O(1)	1.496(2)
P(1)−O(3)	1.584(2)	P(2)−O(9)	1.496(2)
P(2)−O(8)	1.496(2)	P(2)−O(7)	1.576(2)
P(3)−O(14)	1.495(2)	P(3)−O(13)	1.513(2)
P(3)−O(15)	1.567(2)		
Hydrogen Bonds			
O(3)···O(16)#2	2.698(5)	O(4)···O(3W)#3	2.892(5)
O(5)···O(3W)	2.869(6)	O(11)···O(4W)	2.946(6)
O(17)···O(2W)#4	2.773(6)	O(1W)···O(2W)	2.683(5)
O(3W)···O(4W)#5	2.949(6)		
2			
Mn(1)−O(3)#1	2.075(2)	Mn(1)−O(2)	2.106(2)
Mn(1)−N(2)	2.287(3)	Mn(1)−N(4)	2.292(3)
Mn(1)−N(1)	2.315(3)	Mn(1)−N(3)	2.388(3)
Mn(2)−O(1)	2.070(2)	Mn(2)−O(1W)	2.172(3)
Mn(2)−N(6)	2.246(4)	Mn(2)−N(7)	2.282(4)
Mn(2)−N(5)	2.298(4)	Mn(2)−N(8)	2.369(3)
Hydrogen Bonds			
O(4)···O(4W)	2.73(2)	O(5)···O(2W)	2.729(8)
O(6)···O(3W)	2.760(7)	O(1W)···O(3W)#2	2.642(6)
3			
Mn(1)−O(1)	2.033(2)	Mn(1)−O(9)#1	2.067(2)
Mn(1)−O(8)	2.248(2)	Mn(1)−N(2)	2.250(2)
Mn(1)−N(1)	2.250(2)	Mn(2)−O(2)	2.036(2)
Mn(2)−O(7)#1	2.095(2)	Mn(2)−O(8)	2.216(2)
Mn(2)−N(6)	2.245(2)	Mn(2)−N(5)	2.269(2)
Mn(3)−O(3W)	2.169(2)	Mn(3)−O(2W)	2.179(2)
Mn(3)−O(1W)	2.185(2)	Mn(3)−O(4W)	2.199(2)
Mn(3)−N(4)	2.277(3)	Mn(3)−N(3)	2.291(2)
Hydrogen Bonds			
O(3)···O(1W)#2	2.642(3)	O(3)···O(2W)#2	2.708(3)
O(4)···O(3W)	2.758(4)	O(4)···O(6W)#3	2.844(5)
O(5)···O(4W)	2.785(4)	O(6)···O(5W)#3	2.813(5)
O(10)···O(2W)	2.740(3)	O(11)···O(4W)	2.705(4)
O(12)···O(5W)#4	2.740(5)	O(1W)···O(7W)	2.762(4)
O(3W)···O(6W)	2.668(4)	O(5W)···O(7W)	2.766(6)
O(6W)···O(7W)	2.890(7)		
4			
Mn(1)−O(9)	2.019(2)	Mn(1)−O(3)#1	2.097(2)
Mn(1)−O(2)	2.177(2)	Mn(1)−N(3)	2.249(2)
Mn(1)−N(4)	2.266(2)	Mn(2)−O(8)	2.013(2)
Mn(2)−O(1W)	2.195(2)	Mn(2)−N(5)	2.317(2)
Mn(2)−N(6)	2.320(2)	Mn(2)−N(8)	2.324(2)
Mn(2)−N(7)	2.337(2)	Mn(3)−O(7)	2.026(2)
Mn(3)−O(1)#1	2.105(2)	Mn(3)−O(2)	2.191(2)
Mn(3)−N(1)	2.229(2)	Mn(3)−N(2)	2.273(2)
Hydrogen Bonds			
O(1W)···O(2W)	2.700(3)	O(1W)···O(3W)	2.822(3)
O(2W)···O(11)	2.760(6)	O(4)···O(3W)#2	2.793(3)
O(5)···O(3W)#3	2.806(3)		
5			
Mn(1)−O(2)	2.040(2)	Mn(1)−O(1W)	2.180(3)
Mn(1)−N(4)	2.252(3)	Mn(1)−N(1)	2.281(3)
Mn(1)−N(3)	2.287(3)	Mn(1)−N(2)	2.357(3)
Mn(2)−O(1)	2.034(2)	Mn(2)−O(9)#1	2.084(2)
Mn(2)−O(7)	2.169(2)	Mn(2)−N(6)	2.235(3)
Mn(2)−N(5)	2.260(3)	Mn(3)−O(3)#1	2.022(3)
Mn(3)−O(8)#1	2.134(2)	Mn(3)−O(7)	2.148(2)
Mn(3)−N(7)	2.249(3)	Mn(3)−N(8)	2.250(3)
Hydrogen Bonds			
O(10)···O(2W)	2.814(4)	O(10)···O(5W)	2.841(4)
O(11)···O(15W)	2.810(4)	O(11)···O(3W)	2.884(5)
O(2W)···O(7W)	2.700(5)	O(2W)···O(9W)	2.790(5)
O(3W)···O(7W)	2.822(5)	O(3W)···O(8W)#2	2.867(5)
O(4W)···O(5W)	2.767(5)	O(4W)···O(9W)	2.879(5)
O(6W)···O(8W)	2.63(2)	O(7W)···O(9W)#3	2.871(5)
O(9W)···O(15W)#3	2.748(6)		
6			
Mn(1)−O(9)	2.026(2)	Mn(1)−O(13)	2.071(2)
Mn(1)−O(19)	2.182(2)	Mn(1)−N(5)	2.208(3)
Mn(1)−N(6)	2.298(3)	Mn(2)−O(3)	2.020(2)
Mn(2)−O(20)	2.072(2)	Mn(2)−O(15)	2.174(2)
Mn(2)−N(12)	2.198(3)	Mn(2)−N(11)	2.307(3)
Mn(3)−O(7)	2.111(2)	Mn(3)−O(10)#1	2.172(3)
Mn(3)−O(1W)	2.192(3)	Mn(3)−O(2W)	2.228(3)
Mn(3)−N(4)	2.266(3)	Mn(3)−N(3)	2.275(3)
Mn(4)−O(2)	2.036(2)	Mn(4)−O(21)	2.112(2)
Mn(4)−O(15)	2.242(2)	Mn(4)−N(10)	2.247(3)
Mn(4)−N(9)	2.280(3)	Mn(5)−O(1)	2.097(2)
Mn(5)−O(4W)	2.190(3)	Mn(5)−O(3W)	2.216(3)
Mn(5)−O(5)#2	2.219(3)	Mn(5)−N(2)	2.244(3)
Mn(5)−N(1)	2.290(3)	Mn(6)−O(8)	2.040(2)
Mn(6)−O(14)	2.108(2)	Mn(6)−N(7)	2.265(3)
Mn(6)−N(8)	2.268(3)	Mn(6)−O(19)	2.292(2)
Hydrogen Bonds			
O(4)···O(8W)	2.808(4)	O(6)···O(9W)#2	2.799(4)
O(6)···O(6W)	2.839(5)	O(11)···O(7W)	2.715(4)
O(11)···O(5W)	2.786(5)	O(18)···O(8W)	2.644(5)
O(18)···O(5W)#3	2.787(5)	O(24)···O(9W)#4	2.850(5)
O(1W)···O(5W)#1	2.655(4)	O(2W)···O(9W)#5	2.769(5)
O(2W)···O(8W)#6	2.838(4)	O(3W)···O(7W)#4	2.684(5)
O(4W)···O(6W)#2	2.634(4)	O(7W)···O(8W)#7	2.795(6)

[a] Symmetry codes: For **1**: #1 $-x+2, -y+1, -z$; #2 $-x+1, -y+1, -z$; #3 $-x+1, -y+2, -z$; #4 $-x, -y+1, -z+1$; #5 $x+1, y, z$. For **2**: #1 $-x+1, -y, -z$; #2 $x, -y+{}^1/_2, z+{}^1/_2$. For **3**: #1 $-x, -y+1, -z+1$; #2 $x-1, y, z$; #3 $-x+1, -y+2, -z$; #4 $x, y-1, z$. For **4**: #1 $-x$ - 1, $-y-1, -z+1$; #2 $-x-1, -y-1, -z$; #3 $x-1, y-1, z$. For **5**: #1 $-x, -y+1, -z$; #2 $-x+1, -y+1$, -z; #3 $-x+1, -y+1, -z+1$. For **6**: #1 $-x, -y+2, -z$; #2 $-x+1, -y+1, -z+1$; #3 $x, y, z+1$; #4 $-x+1, -y+1, -z$; #5 $x-1, y+1, z$; #6 $-x, -y+2, -z+1$; #7 $x, y, z-1$.

The hydrogen atoms for the water molecules except those in **4** are not included in the refinements. The ClO_4^- anion in **2** is severely disordered, and two of its oxygen atoms (O(43), O(44)) each display two orientations with 50% occupancy for each site. One sulfonate group in **4** is also severely disordered, and three sulfonate oxygen atoms (O(10), O(11), O(12)) each display two orientations with 50% occupancy for each site. The disordered lattice water molecules in compound **3** (O(8w), O(9w)) and compound **5** (O(6w)) also display two orientations with 50% occupancy for each site. The occupancy factors of O(2w) to O(4w) in **2** and O(10w) to O(13w) in **5** were reduced to 50% as a result of their larger thermal parameters. Crystallographic data and structural refinements for **1**−**6** are summarized in Table 1. Important bond lengths are listed in Table 2. More details on the crystallographic studies as well as atom displacement parameters are given in the Supporting Information.

Scheme 1. Comparison and Relationship between Cluster Cores in **1**−**6**[a]

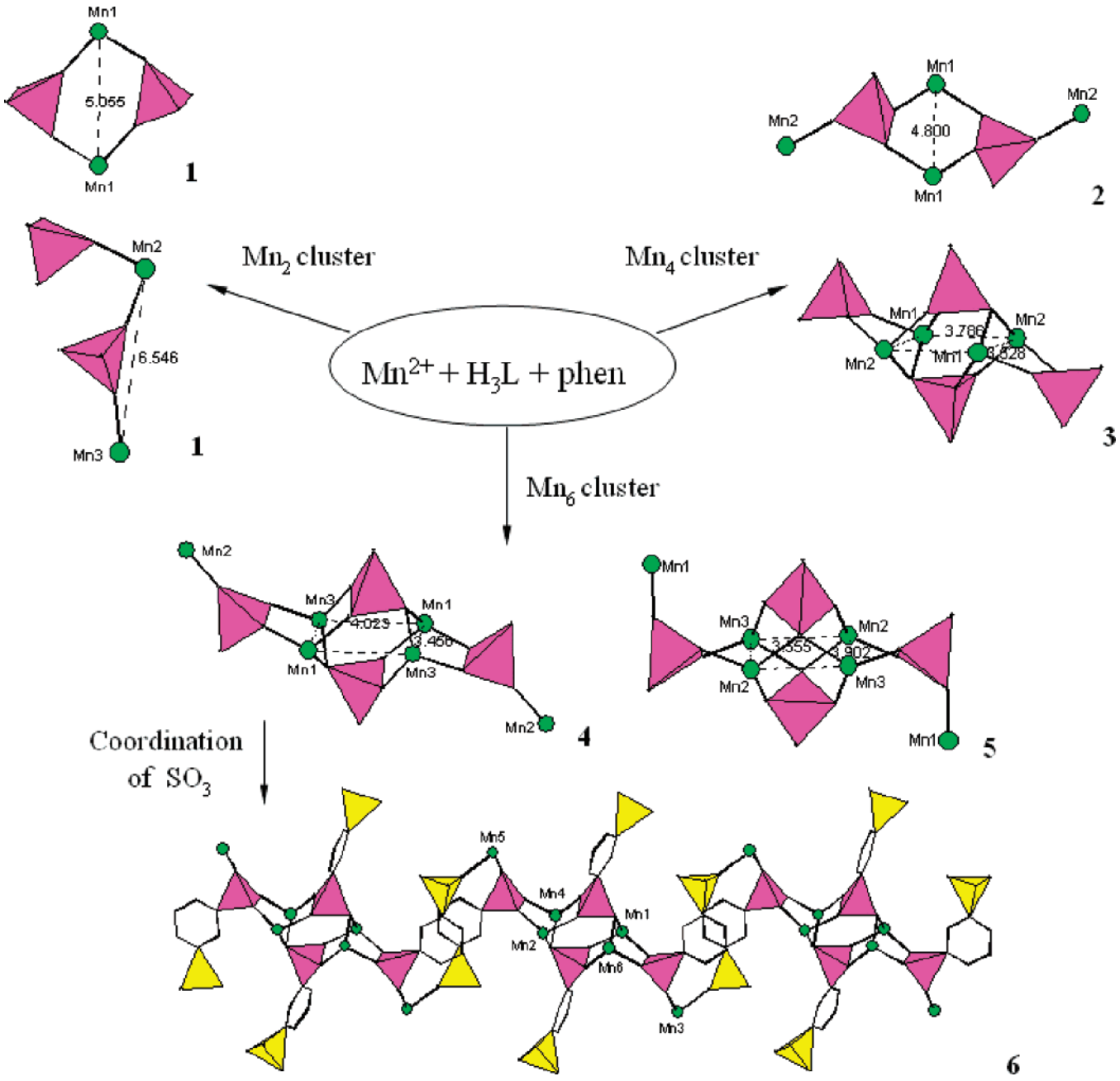

[a] The CPO_3 and CSO_3 groups are represented by pink and yellow, respectively.

Results and Discussion

Hydrothermal reactions of manganese(II) salts with *m*-sulfophenylphosphonic acid (*m*-$HO_3S-Ph-PO_3H_2$, H_3L) and 1,10-phenanthroline (phen) afforded six novel manganese(II) sulfonate−phosphonates, namely, $[Mn_2(HL)_2(phen)_4]$-$[Mn_2(HL)_2(phen)_4(H_2O)]_2 \cdot 6H_2O$ (**1**), $[Mn_4(L)_2(phen)_8(H_2O)_2]$-$[ClO_4]_2 \cdot 3H_2O$ (**2**), $[Mn(phen)(H_2O)_4]_2[Mn_4(L)_4(phen)_4] \cdot 10H_2O$ (**3**), $[Mn_6(L)_4(phen)_8(H_2O)_2] \cdot 4H_2O$ (**4**), $[Mn_6(L)_4$-$(phen)_8(H_2O)_2] \cdot 24H_2O$ (**5**), and $[Mn_6(L)_4(phen)_6(H_2O)_4] \cdot 5H_2O$ (**6**). They represent the first metal phosphonate clusters based on purely manganese(II) metal centers. Their structures feature five types of clusters (Scheme 1). It is found that the cluster compounds isolated depend on many factors such as the counter anions of manganese salts, the coordination mode of the phosphonate ligand adopted, and the molar ratios of the reactants as well as the pH value of the reaction media. When the counteranion is present in the compound as in **2**, the charge on the cluster unit is altered; the pH value of the reaction media affects the degree of the protonation of the sulfonate−phosphonate ligand and also the coordination mode it adopts; and the amount of phen ligand used in the preparation may change the coordination environment around the surface manganese(II) ions of the cluster unit. Our studies also indicate that the amorphous products or/and phase mixtures will be obtained when the reactions were not carried

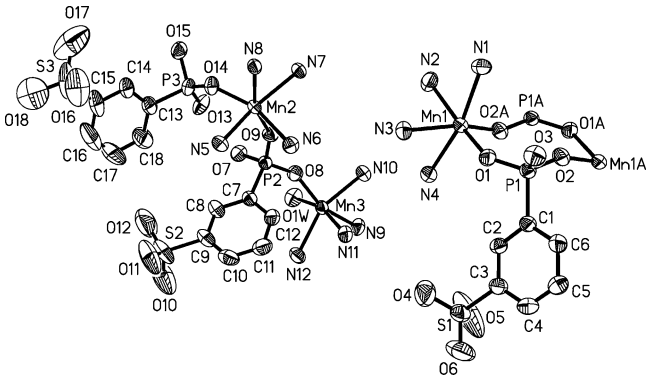

Figure 1. ORTEP representation of the selected unit of **1**. The thermal ellipsoids are drawn at 50% probability. Lattice water molecules and carbon atoms of the phen ligands have been omitted for clarity. Symmetry codes for the generated atoms: a. $-x + 2, -y + 1, -z$.

out under the optimum conditions described in the experimental section.

Structural Descriptions. 1 contains a dinuclear $[Mn_2(HL)_2(phen)_4]$ and two dinuclear $[Mn_2(HL)_2(phen)_4(H_2O)]$ clusters as well as six lattice water molecules. There are three unique manganese(II) ions in the asymmetric unit of **1** (Figure 1). Both the Mn(1) and Mn(2) ions are six-coordinate with two phosphonate oxygen atoms from two HL^{2-} anions as well as two bidentate chelating phen ligands. The Mn(3) ion is six-coordinate with one phosphonate oxygen atom and two bidentate chelating phen ligands as well as an aqua ligand. The Mn−O (2.066(2)−2.182(3) Å) and Mn−N (2.253(2)−2.345(3) Å) distances are comparable to those reported in other manganese(II) phosphonates.[10,11]

There are three unique HL^{2-} ligands in **1**. The phosphonate groups of these ligands are singly protonated, as indicated by a much-longer P−O bond (Table 2). The ligand containing P(1) and S(1) atoms or P(2) and S(2) atoms is bidentate and bridges with two manganese(II) ions via its two phosphonate oxygen atoms. The third sulfonate−phosphonate ligand containing P(3) and S(3) is monodentate and connects with a manganese(II) center by using one of its phosphonate oxygen atoms (O(14)). All of the sulfonate groups of the ligands remain non-coordinated. A pair of manganese(1) ions is bridged by two HL^{2-} ligands into a ringlike $[Mn_2(HL)_2(phen)_4]$ dinuclear cluster unit with a Mn_2P_2 four member ring (part a of Figure 2), whereas one Mn(2) ion and one Mn(3) ion are bridged by one HL^{2-} ligand into an open $[Mn_2(HL)_2(phen)_4(H_2O)]$ dinuclear cluster (part b of Figure 2). The Mn···Mn separation within the $[Mn_2(HL)_2(phen)_4]$ cluster (5.055(4) Å) is much shorter than that in the $[Mn_2(HL)_2(phen)_4(H_2O)]$ dinuclear cluster (6.546(13) Å). The shortest intercluster Mn···Mn separation is at least 7.539(1) Å.

The above two types of dinuclear clusters in **1** are assembled into a 3D supramolecular network via hydrogen bonds as well as weak $\pi\cdots\pi$ interactions (Table 2, Figure S2 and Table S1 in the Supporting Information). The lattice water molecules are located at the voids of the structure. A number of hydrogen bonds are formed among water molecules, non-coordinated phosphonate, and sulfonate oxygen atoms. The O···O contacts range from 2.683(5) to 2.949(6) Å.

2 features a tetranuclear $[Mn_4(L)_2(phen)_8(H_2O)_2]^{2+}$ cluster. There are two unique manganese(II) ions in its asymmetric unit (Figure 3). The Mn(1) ion is six-coordinate with two phosphonate oxygen atoms from two L^{3-} anions as well as two bidentate chelating phen ligands, whereas the Mn(2) ion is six-coordinate with one phosphonate oxygen atom and two bidentate chelating phen ligands as well as an aqua ligand. The Mn−O (2.070(2)−2.172(3) Å) and Mn−N (2.246(4)−2.388(3) Å) distances are comparable to those in **1** and other reported manganese(II) phosphonates.[10,11]

The L^{3-} ligands in **2** are tridentate. Each of them bridges with three manganese(II) ions via its three phosphonate oxygen atoms (Scheme 2). Two Mn(1) ions and two Mn(2) ions are bridged by two L^{3-} ligands into a tetranuclear cluster (Scheme 1). Such a cluster can be viewed as derived from the ringlike dinuclear manganese(II) cluster in **1** through the coordination of the third phosphonate oxygen atoms of its two bidentate HL^{2-} ligands (Figure 4). The Mn···Mn separations within the tetranuclear cluster unit are 4.800(2), 5.634(2), and 6.552(4) Å. Such a tetranuclear cluster is significantly different from that in $[Zn_4(L)_4(phen)_4][Zn(phen)_3]_2\cdot 20H_2O$ in that the metal···metal distances in the latter are much shorter due to the tetradentate bridging coordination mode adopted by the phosphonate−sulfonate ligands.[7h] The two positive charges of the $[Mn_4(L)_2(phen)_8(H_2O)_2]^{2+}$ cation are compensated by two ClO_4^- anions. These discrete tetranuclear clusters in **2** are assembled into a 3D supramolecular network via hydrogen bonds as well as weak $\pi\cdots\pi$ interactions (Table 2, Figure S3 and Table S1 in the Supporting Information). The shortest intercluster Mn···Mn contact is 8.513(1) Å. The ClO_4^- anions and lattice water molecules are located at the voids of the structure. A number of hydrogen bonds are formed among lattice water molecules and sulfonate oxygen atoms. The O···O contacts range from 2.642(6) to 2.760(7) Å.

3 contains a tetranuclear cluster of $[Mn_4(L)_4(phen)_4]^{4-}$ anion and two isolated $[Mn(phen)(H_2O)_4]^{2+}$ cations as well as 10 lattice water molecules. There are three unique manganese(II) ions in its asymmetric unit (Figure 5). Both Mn(1) and Mn(2) are five-coordinate with three phosphonate oxygen atoms from three L^{3-} anions as well as a bidentate chelating phen ligand. The Mn(3) ion is six-coordinate with a bidentate chelating phen ligand as well as four aqua ligands. The Mn−O (2.033(2)−2.248(2) Å) and Mn−N (2.245(2)−2.291(2) Å) distances are comparable to those in **1**−**2** and other reported manganese(II) phosphonates.[10,11]

There are two types of L^{3-} ligands in **3**. The one containing P(1) and S(1) atoms is bidentate and bridges with two manganese(II) ions via its two phosphonate oxygen atoms. The L^{3-} ligand containing P(2) and S(2) is tetradentate and bridges with four manganese(II) ions by using its three phosphonate oxygen atoms (Scheme 2). The O(8) atom acts as a μ^2-bridging metal linker. Two Mn(1) ions and two Mn(2) ions are bridged by four L^{3-} ligands into a cagelike tetranuclear cluster unit (Scheme 2). The four manganese(II) ions form a slightly distorted rectangle. The two

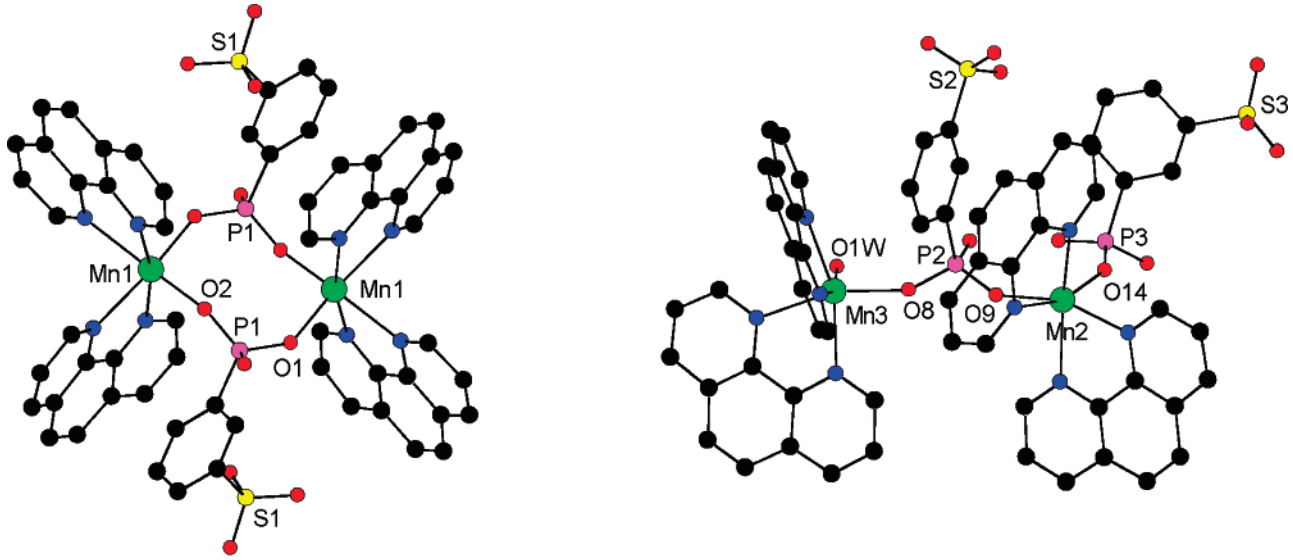

Figure 2. Dimeric cluster units in **1**. Manganese, phosphorus, sulfur, oxygen, nitrogen, and carbon atoms are drawn as green, pink, yellow, red, blue, and black circles, respectively.

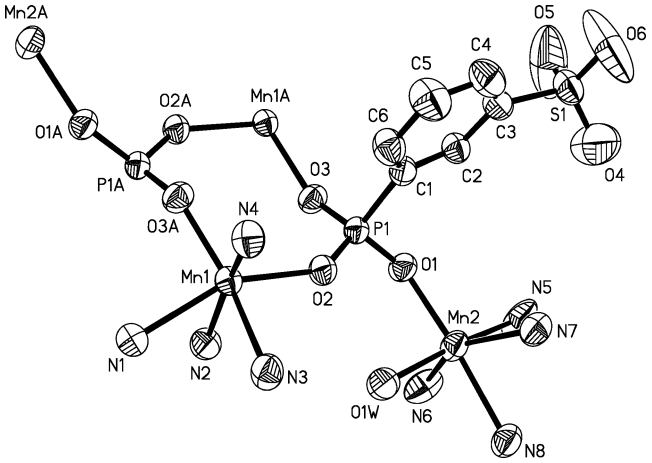

Figure 3. ORTEP representation of the selected unit of **2**. The thermal ellipsoids are drawn at 50% probability. Lattice water molecules and ClO_4^- anions and carbon atoms of the phen ligands have been omitted for clarity. Symmetry codes for the generated atoms: a. $-x + 1, -y, -z$.

Scheme 2 Coordination Modes of *m*-Sulfophenylphosphonic Acid Found in **1**−**6**

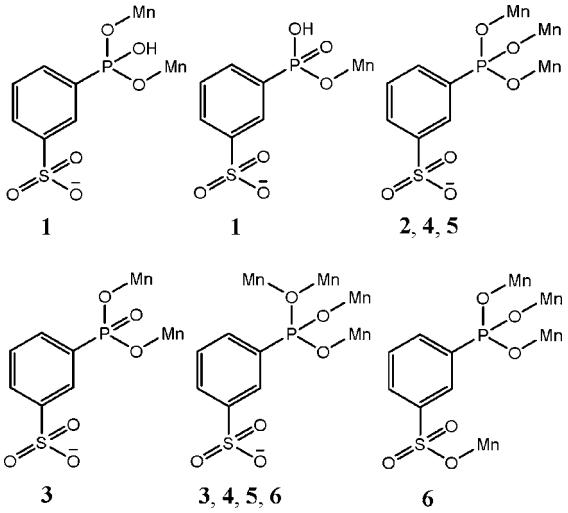

Mn···Mn edges are 3.528(15) and 3.786(15) Å, respectively. The Mn−Mn−Mn angles of 90.5 and 89.5 are close to ideal 90°. The diagonal Mn···Mn contacts within the cluster are 5.155(6) and 5.196(7) Å, respectively. The shortest Mn···Mn distance from the isolated Mn(3) ion to the tetranuclear cluster is 6.928(1) Å. Neighboring tetranuclear clusters are well separated with a minimum intercluster Mn···Mn contact of 8.897(1) Å. The two tetradentate phosphonate groups cap above and below the central Mn_4 rectangle, whereas the two bidentate phosphonate groups serve as bridging ligands on the two short Mn···Mn edges from the left and right sides, respectively (Figure 6). Such a tetranuclear cluster unit is similar to the tetranuclear cluster in $[Zn_4(L)_4(phen)_4][Zn(phen)_3]_2 \cdot 20H_2O$.[7h] Compared with the Mn_4 cluster in **2**, the Mn_4 cluster in **3** is much more contracted.

The four negative charges of the $[Mn_4(m\text{-}O_3S{-}Ph{-}PO_3)_4(phen)_4]^{4-}$ anion are compensated by two $[Mn(phen)(H_2O)_4]^{2+}$ cations. These discrete clusters and $[Mn(phen)(H_2O)_4]^{2+}$ cations in **3** are assembled into a 3D supramolecular network via hydrogen bonds as well as $\pi\cdots\pi$ packing interactions. (Table 2, Figure S4 and Table S1 in the Supporting Information). A large number of hydrogen bonds are formed among lattice water molecules, non-coordinated phosphonate, and sulfonate oxygen atoms. The O···O contacts range from 2.642(3) to 2.890(7) Å.

The formulas of $([Mn_6(L)_4(phen)_8(H_2O)_2]\cdot 4H_2O$ (**4**) and $[Mn_6(L)_4(phen)_8(H_2O)_2]\cdot 24H_2O$ (**5**) differ only in the number of lattice water molecules. Their structures feature two types of slightly different isolated hexanuclear manganese(II) clusters. Among the three independent manganese atoms in **4** and **5**, two of them are five-coordinate with three phosphonate oxygen atoms from three L^{3-} anions as well as a bidentate chelating phen ligand; the third one is six-coordinate with one phosphonate oxygen atom and two bidentate chelating phen ligands as well as an aqua ligand.

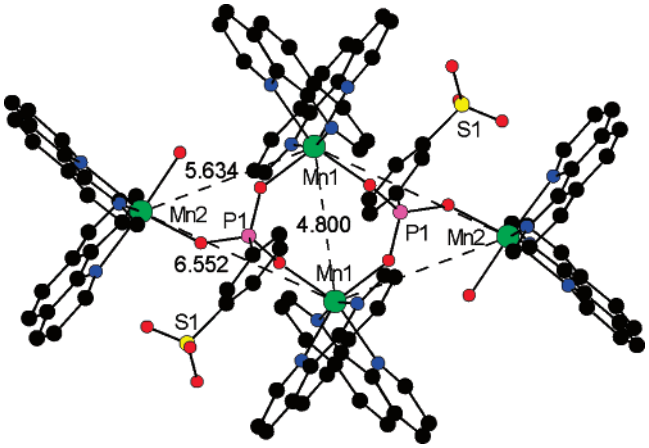

Figure 4. Tetranuclear cluster unit in **2**. Manganese, phosphorus, sulfur, oxygen, nitrogen, and carbon atoms are drawn as green, pink, yellow, red, blue, and black circles, respectively.

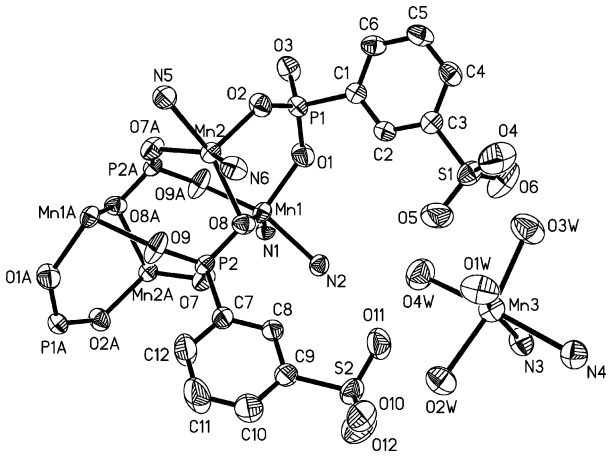

Figure 5. ORTEP representation of the selected unit of **3**. The thermal ellipsoids are drawn at 50% probability. Lattice water molecules and carbon atoms of the phen ligands have been omitted for clarity. Symmetry codes for the generated atoms: a. $-x, -y + 1, -z + 1$.

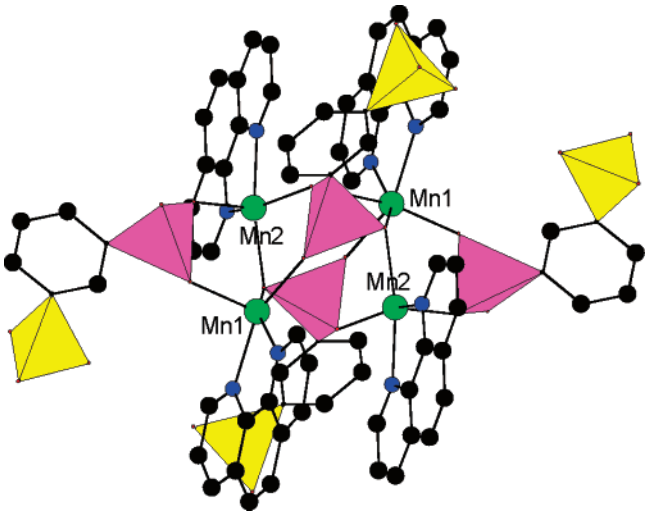

Figure 6. Tetranuclear manganese(II) cluster in **3**. The CPO_3 and CSO_3 groups are shaded in pink and yellow, respectively. Manganese, nitrogen, and carbon atoms are drawn as green, blue, and black circles, respectively.

The Mn−O (2.013(2)−2.191(2) Å) and Mn−N (2.229(2)−2.357(3) Å) distances are comparable to those in **1**−**3** and other reported manganese(II) phosphonates.[10,11]

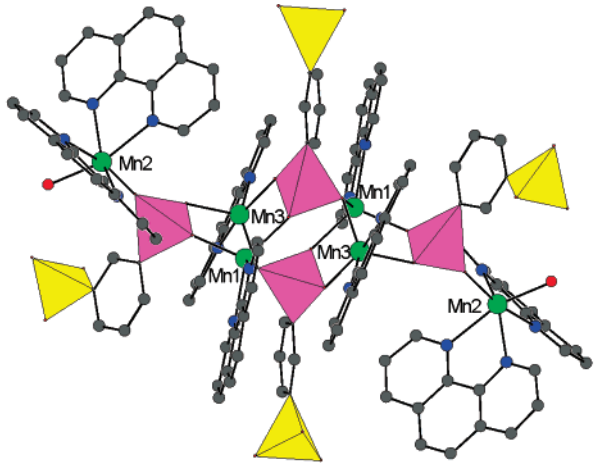

(a)

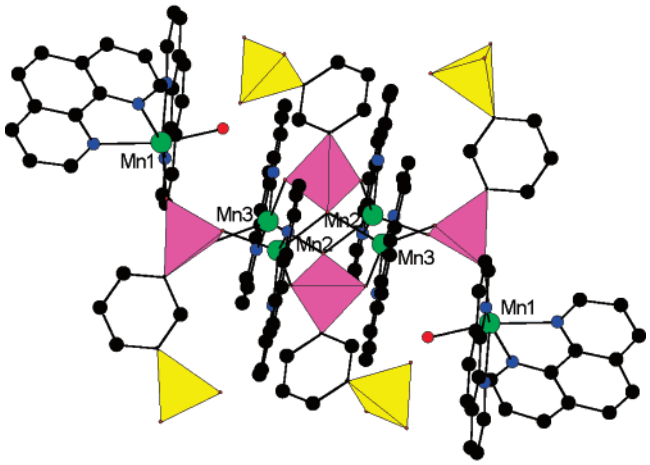

(b)

Figure 7. Hexanuclear cluster units in **4** (a) and **5** (b). The CPO_3 and CSO_3 groups are shaded in pink and yellow, respectively. Manganese, oxygen, nitrogen, and carbon atoms are drawn as green, red, blue, and black circles, respectively.

The four L^{3-} ligands in **4**−**5** adopt two types of coordination modes. One is tetradentate and bridges with four manganese(II) ions using its three phosphonate oxygen atoms. The second type is tridentate in which each phosphonate oxygen atom connects with one manganese(II) ion (Scheme 2). The interconnection of six manganese(II) ions by the above two types of L^{3-} anions resulted in two slightly different hexanuclear clusters. The one in **4** can be considered as derived from the tetranuclear manganese(II) cluster in **3** through the coordination of the third phosphonate oxygen atoms of its two bidentate L^{3-} ligands (Scheme 2). The cluster in **5** can be viewed as derived from that of **4** through distortion (Figure 7). The main difference is that the Mn···Mn edge bridged by μ^2-O in **4** connects with three L^{3-} ligands, whereas that in **5** links with four L^{3-} ligands (Scheme 1). Another difference is that the cluster in **5** is much more contracted than that in **4**; hence, it resulted in different intracluster Mn···Mn separations (Figure 8). Therefore, the cluster unit of **5** can be built from that of **4** by rotating the two tetradentate capping L^{3-} anions about 90° along the axis perpendicular to the central Mn_4 plane. The

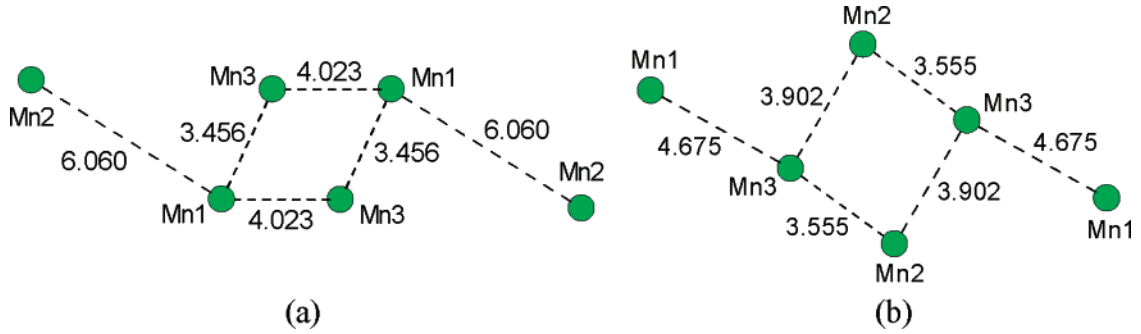

Figure 8. The Mn_6 cluster cores in **4** (a) and **5** (b) with the labeling of some Mn···Mn distances.

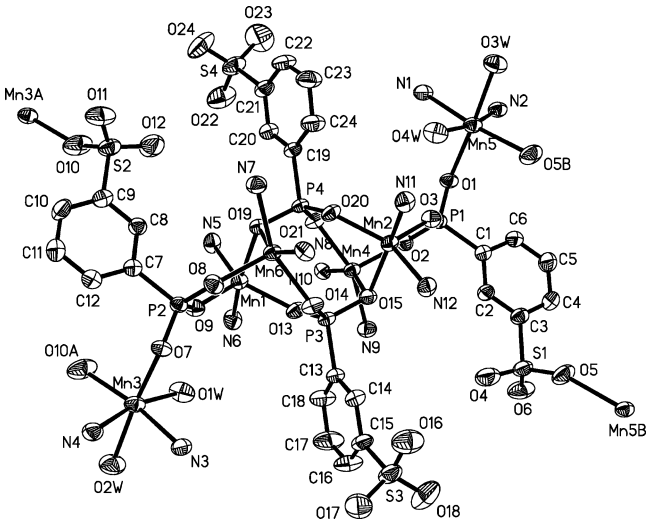

Figure 9. ORTEP representation of the selected unit of **6**. The thermal ellipsoids are drawn at 50% probability. Lattice water molecules and carbon atoms of the phen ligands have been omitted for clarity. Symmetry codes for the generated atoms: a. $-x, 2-y, -z$; b. $1-x, 1-y, 1-z$.

two Mn···Mn edges of the central Mn_4 square are very close in both compounds, but the Mn(1)···Mn(3) distance of 4.68(2) Å within the Mn_6 cluster in **5** is significantly shorter than the corresponding Mn(2)···Mn(1) distance of 6.060(4) Å in **4**. The six manganese(II) ions in both **4** and **5** form a Mn_6 ring in the chair conformation, which is similar to our previously reported hexanuclear cluster units in zinc(II) sulfonate−phosphonates.[7h]

The discrete clusters in **4** and **5** are also assembled into a 3D supramolecular network via hydrogen bonds as well as $\pi\cdots\pi$ packing interactions. (Table 2; Figures S5, S6, and Table S1 in the Supporting Information). The lattice water molecules are located at the cavities of the structure. A number of hydrogen bonds are formed among lattice water molecules and sulfonate oxygen atoms.

6 features a 1D chain based on hexanuclear manganese(II) clusters (Figure 9). There are six unique manganese(II) ions in its asymmetric unit. Both the Mn(1) and the Mn(2) ions are five-coordinate with three phosphonate oxygen atoms from three L^{3-} anions as well as a bidentate chelating phen ligand. The Mn(4) ion and Mn(6) ions are six-coordinate with four phosphonate oxygen atoms from three L^{3-} anions as well as a bidentate chelating phen ligand, whereas the Mn(3) and Mn(5) ions are six-coordinate with one phosphonate oxygen atom and one sulfonate oxygen atom from two L^{3-} anions as well as a bidentate chelating phen ligand and two aqua ligands. The Mn−O (2.020(2)−2.292(2) Å) and Mn−N (2.208(3)−2.307(3) Å) distances are comparable to those in **1**−**5**.

The four L^{3-} ligands adopt two types of coordination modes. The ligand containing P(3) and S(3) or P(4) and S(4) is tetradentate and bridges with four manganese(II) ions using their three phosphonate oxygen atoms. O(15) and O(19) atoms act as a μ^2-bridging ligand. The sulfonate groups remain non-coordinated. Such a coordination mode is also found in **4** and **5**. The ligand containing P(1) and S(1) or P(2) and S(2) is tetradentate and bridges with four manganese(II) ions by using their three phosphonate oxygen atoms and one sulfonate oxygen atom (Scheme 2). The interconnection of six manganese(II) ions via bridging phosphonate groups of the phosphonate−sulfonate ligand led to a hexanuclear cluster, which is similar to that in **4**. Neighboring such clusters are bridged by phosphonate−sulfonate ligands via S−O−Mn bridges into a 1D chain along the diagonal of the *a* and *c* axes (Figure 10). The four edges of the central Mn_4 square are 3.506(1), 3.520(1), 3.812(1), and 3.892(1) Å, respectively, which are close to those in **4**. The shortest Mn···Mn distances between the side manganese(II) ions and the central Mn_4 square within a Mn_6 cluster is 5.380(1) Å, which are somewhat shorter than that in **4**. The nearest intercluster Mn···Mn separation within the 1D chain is 8.759(6) Å, which is close to the shortest intercluster Mn···Mn distance in **4** (8.777(1) Å). These 1D chains in **6** are further interconnected via hydrogen bonds as well as $\pi\cdots\pi$ packing interactions into a 3D network (Table 2, Figure S1 and Table S1 in the Supporting Information). The lattice water molecules are located at the cavities of the structure. A number of hydrogen bonds are formed among the non-coordinated sulfonate oxygen atoms and the lattice water molecules. The O···O contacts range from 2.634(4) to 2.850(5) Å.

Magnetic Property Studies. The dc magnetic properties for **1**−**6** were measured in the temperature range of 2−300 K at the applied magnetic field of 1000 Oe (Figure S8 in the Supporting Information). At 300 K, the effective magnetic moments (μ_{eff}) for **1**−**6** are measured to be 14.43, 11.82, 13.85, 13.79, 13.72, and 13.86 μ_B, respectively, which are slightly smaller than the theoretical values for the four or six isolated magnetic centers per formula unit (14.49 μ_B for **1** and **3**−**6**; 11.83 μ_B for **2**). Upon cooling down over the whole temperature range, the μ_{eff} values for **1**−**6** are decreased and reached 9.88, 7.91, 8.02, 7.85, 8.52, and 8.49 μ_B, respectively, at 2.0 K, indicating the antiferromagnetic

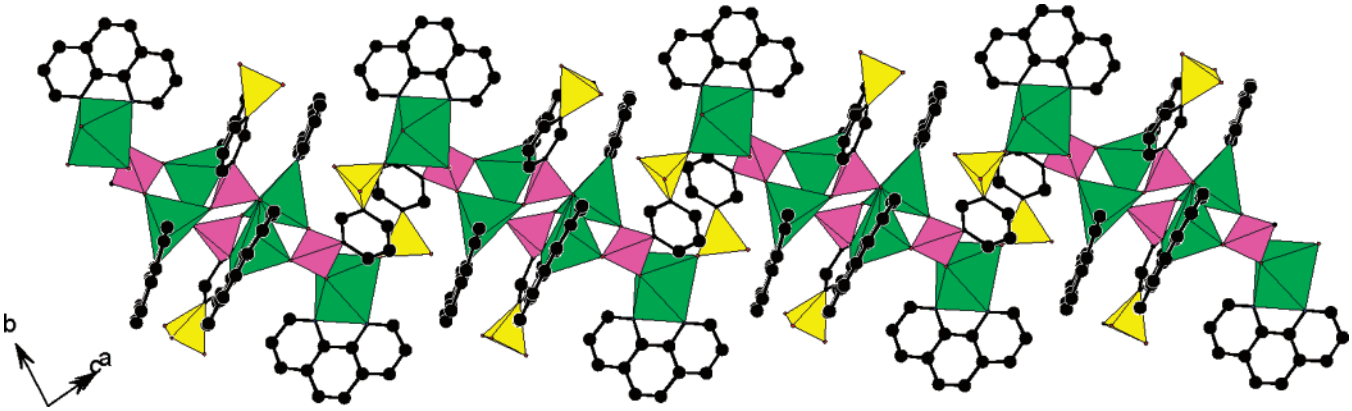

Figure 10. 1D chain based on hexanuclear Mn_6 clusters in **6**. The MnO_xN_y, CPO_3, and CSO_3 groups are shaded in green, pink, and yellow, respectively.

Table 3. Fitting Parameters of Magnetic Susceptibility for **1**−**6**

compound	fitting Mn^{2+} model (according to the unit-cell)	dominant Mn^{2+} to Mn^{2+} connection	J (cm^{-1})	g
1	3 dimers	−O−P−O−	−0.16	2.0
2	dimer + 2 isolated Mn	2×(−O−P−O−)	−0.7	2.0
3	2 dimers + 2 isolated Mn	−O−	−2.1	1.95
4	2 dimers + 2 isolated Mn	−O−	−2.7	1.95
5	2 dimers + 2 isolated Mn	−O−	−1.9	1.93
6	2 dimers + 2 isolated Mn	−O−	−2.6	1.96

interactions between magnetic centers in all six compounds. It is expected that such antiferromagnetic interactions occur mainly between magnetic centers within the cluster units. Magnetic interactions between cluster units are expected to be negligible because these cluster units are well separated as discussed in crystal structure sections. It is noted that **3**−**6** each contains two Mn_2 dimers, in which each pair of manganese(II) ions is bridged by a μ^2-phosphonate oxygen atom with Mn···Mn distances less than 3.600(1) Å. Each pair of manganese(II) ions of the Mn_2 dimers in **1** and **2** is interconnected via O−P−O bridges with much longer Mn···Mn separations (>4.815(1) Å). The other two manganese(II) ions in **2** and **4**−**6** are well separated from the dimers and hence can be considered as isolated. Therefore, the χT values of all six compounds can be fitted with the combination of dimers and isolated Mn^{2+} ions. The magnetism of the Mn^{2+} dimers is fitted to the Hamiltonian ($H = -2JS_1S_2$) and isolated Mn^{2+} ions are approximated by the Curie or Curie−Weiss law with small Weiss Constants. The variable-temperature magnetic susceptibility data for these compounds were fitted to the modified Van Vleck equation using the isotropic exchange Hamiltonian ($H = -2JS_1S_2$) for two interacting $S = {}^5/_2$ centers:[15]

$$\chi_{\mathrm{dim}} = \frac{2Ng^2\beta^2}{kT} \cdot \frac{e^x + 5e^{3x} + 14e^{6x} + 30e^{10x} + 55e^{15x}}{1 + 3e^x + 5e^{3x} + 7e^{6x} + 9e^{10x} + 11e^{15x}} \quad (1)$$

where $x = 2J/kT$. These models produced a good fit to the experimental data at most of the temperature range. Parameters and models for the magnetic fitting are listed in the Table 3. The obtained J value is comparable to the values reported for the other dinuclear manganese complexes.[16] The much-more negative J values for **3**−**6** compared with those of **1**−**2** indicate much-stronger magnetic interactions in **3**-**6**, which are in agreement with larger intracluster Mn···Mn separations in **1**−**2** compared with those of the remaining ones.

TGA Studies. TGA curves of **1** exhibit three main steps of weight losses (Figure S9). The first step started at 40 °C and completed at 203 °C, which corresponds to the release of eight water molecules. The observed weight loss of 3.6% matches well with the calculated value (3.6%). The second step (236−512 °C) and the third step (512−830 °C) are overlapping, which correspond to the combustion of the organic ligands. The total observed weight loss is 78.6%, and the final residuals were not characterized. TGA curves of **2** exhibit three main steps of weight losses. The first step started at 40 °C and completed at 149 °C, which corresponds to the release of eight water molecules. The observed weight loss of 3.8% is very close to the calculated value (3.7%). The second step (194−336 °C) and the third step (336−733 °C) are overlapping, which correspond to the combustion of the phen, ClO_4^- anion, and sulfonate−phosphonate ligands. The total weight loss is 80.9% and the final residuals were not characterized. TGA curves of compound **3** exhibit three main steps of weight losses. The first step started at 40 °C and completed at 153 °C, which corresponds to the release of 18 water molecules. The observed weight loss of 11.5% is close to the calculated value (12.1%). The second step (296−518 °C) and the third step (518−623 °C) are overlapping, which correspond to the combustion of the phen and sulfonate−phosphonate ligands. The total weight loss is 72.1%, and the final residuals were not characterized. TGA curves of **4** exhibit three main steps of weight losses. The first step started at 103 °C and completed at 185 °C, which corresponds to the release of six water molecules. The observed weight loss of 3.9% is very close to the calculated value (3.8%). The second step (410−554 °C) and the third step (554−724 °C) are overlapping, which correspond to the combustion of the phen and sulfonate−phosphonate ligands.

(15) Kahn, O. *Molecular Magnetism*; VCH Publishers, Inc.: New York, 1993.

(16) (a) Fuller, A. L.; Watkins, R. W.; Dunbar, K. R.; Prosvirin, A. V.; Arifc, A. M.; Berreau, L. M. *Dalton Trans.* **2005**, 1891. (b) Ishida, T.; Kawakami, T.; Mitsubori, S.; Nogami, T.; Yamaguchi, K.; Iwamura, H. *J. Chem. Soc., Dalton Trans.* **2002**, 3177. (c) Durot, S.; Policar, C.; Pelosi, G.; Bisceglie, F.; Mallah, T.; Mahy, J. P. *Inorg. Chem.* **2003**, *42*, 8072. (d) Mukherjee, P. S.; Konar, S.; Zangrando, E.; Mallah, T.; Ribas, J.; Chaudhuri, N. R. *Inorg. Chem.* **2003**, *42*, 2695.

The total observed weight loss is 74.4%, and the final residuals were not characterized. TGA curves of **5** show three main steps of weight losses. The first step started at 42 °C and completed at 172 °C, which corresponds to the release of 26 water molecules. The observed weight loss of 13.0% is slightly smaller than the calculated value (14.7%). The second step (275−568 °C) and the third step (568−695 °C) are overlapping, which correspond to the combustion of the organic ligands. The total observed weight loss is 77.0%, and the final residuals were not characterized. TGA curves of **6** indicate three main steps of weight losses. The first step started at 40 °C and completed at 185 °C, which corresponds to the release of 9 water molecules. The observed weight loss of 5.9% is close to the calculated value (6.5%). The second step (407−533 °C) and the third step (533−657 °C) are overlapping, which correspond to the combustion of the phen and sulfonate−phosphonate ligands. The total observed weight loss is 71.7%, and the final residuals were not characterized.

Conclusion

In summary, the syntheses, crystal structures, and magnetic properties of six novel manganese(II) sulfonate−phosphonates with dinuclear, tetranuclear, or hexanuclear cluster units have been reported. It is noted that the nature of the clusters formed is strongly affected by the counter anions of the manganese(II) sources and the reaction pH values as well as the molar ratio of reactants. Higher pH values in the Mn^{2+}-H_3L-phen system normally lead to stronger coordination ability of the sulfonate−phosphonate ligand to the metal centers and the formation of higher nuclear clusters, as indicated by those of **3**−**6** compared with **1** and **2**. **1** contains two types of dinuclear manganese(II) clusters. **2** and **3** feature two types of tetranuclear manganese(II) clusters, whereas **4** and **5** exhibit two types of hexanuclear manganese(II) clusters. **6** features a 1D chain based on hexanuclear manganese(II) clusters similar to that in **4**. The geometries of these different clusters are strongly related to the different coordination modes of the sulfonate−phosphonate ligands adopted. It is anticipated that many other cage compounds based on metal phosphonates can be synthesized by using such a synthetic route.

Acknowledgment. This work is supported by National Natural Science Foundation of China (Grant 20521101), NSF of Fujian Province (Grants E0420003 and E0610034), and the Key Project of Chinese Academy of Sciences (Grant KJCX2-YW-H01). We thank Prof. Kim Dunbar at Texas A & M University for her help with the magnetic property measurements.

Supporting Information Available: X-ray crystallographic files in CIF format, $\pi\cdots\pi$ packing interactions, 3D packing diagrams, and simulated and experimental XRD patterns for all six compounds. This material is available free of charge via the Internet at http://pubs.acs.org.

IC701213G